RSC Advances

ROYAL SOCIETY OF CHEMISTRY

www.rsc.org/advances

Reactive force field simulation on the polymerization and hydrolytic reaction in the calcium aluminate silicate hydrate (C-A-S-H) gel: structure, dynamics and mechanical properties

Dongshuai HOU[a] Zongjin LI[b] Tiejun ZHAO[c]

a. Assistant Professor; Qingdao Technological University(Cooperative Innovation Center of Engineering Construction and Safety in Shandong Blue Economic Zone), Qingdao, China; Corresponding author, telephone number: +85267636710; email address: dhou@ust.hk ; monkeyphil@126.com

b. Professor; Qingdao Technological University(Cooperative Innovation Center of Engineering Construction and Safety in Shandong Blue Economic Zone), Qingdao, China; zongjin@ust.hk

c. Professor, Qingdao Technological University(Cooperative Innovation Center of Engineering Construction and Safety in Shandong Blue Economic Zone), Qingdao, China; ztjgp@263.net

Abstract

Reactive force field was first utilized to characterize the structure, dynamic and mechanical properties of calcium-aluminate-silicate-hydrate, which is essential in the chemistry of high alumina and layered gel in the Portland cement. In order to study the role of Al atoms, the properties of Al atoms located in the calcium silicate sheet and the interlayer region have been investigated. The Si-Al substitution in the calcium silicate sheet has not changed the layered structure of C-A-S-H gel. On the other hand, the Al atoms, presence in the interlayer region, improve the structure and mechanical performance significantly. Connectivity factor, Q species evolution indicates that the aluminate species in the interlayer region plays an essential role in bridging the defective silicate chains and transforming the layered C-A-S-H gel at low Al/Ca level to the branch network structure at high Al/Ca level. The structural transition is partly attributed to the aluminate-silicate connection by the NBO sites and is partly caused by the polymerization reaction between the aluminate species, both of which can be described by the Reactive Force Field. Additionally, the polymerization reaction by the aluminate species also leads to hydrolytic reaction. In this way, a lot of water molecules are transformed to hydroxyls, even bridging oxygen atoms. Dynamically, due to the strong strength of the Al-O bond, the aluminate-silicate network in C-A-S-H gel has better stability at higher Al/Ca ratios. Furthermore, uniaxial tension tests on the C-A-S-H gels, demonstrate the mechanical behavior and large structural deformation of the gel. Both Young's modulus and the tensile strength are improved significantly with increasing aluminum content, indicating good loading resistance ability in the aluminate-silicate network. The tensile deformation, simulated by the reactive force field, is also coupled with de-polymerization of aluminate species and the water dissociation reaction, which shows good plasticity due to the Al atoms addition.

Key words: aluminum substitution, reactive force field, aluminate-silicate network, polymerization, water dissociation.

1. Introduction

Concrete is the most widely utilized construction and building material in modern cities and the manufacturing process of concrete is closely related with the environment. Unfortunately, the production of traditional Portland cement results in significant release of CO_2 and other greenhouse gases [1]. Hence, environmental friendliness acts as the leading issue in the sustainable development of the cement and concrete industry. In particular, mineral admixtures, partially substituting the cement materials, provide a promising way to reuse industrial waste and reduce energy consumption. Due to its pozzolanic properties, furnace slag and fly ash can be used as a replacement for some of the Portland cement content of concrete [2] [3]. Since the content of the furnace slag and fly ash include some aluminate phases, the hydration reaction produces calcium-aluminate-silicate-hydrate (C-A-S-H) gel, like the Calcium-Silicate-Hydrate (C-S-H) gel in the OPC cement [4] [5] [6].

C-A-S-H gel, as the main hydration product, is responsible for the mechanical properties and durability of the materials. The introduction of aluminate species can effectively improve the chemical stability, mechanical and transport properties of traditional binding phase, C-S-H gel. Recently, the archaeologists excavated the old concrete constructed at Roman period from the ocean near Naples [7] [8]. Despite of thousands of years' immersing in the sea water, the structure of concrete remained integrity, exhibiting very good durability. It is worth noting that the main hydration product in the old concrete is C-A-S-H gel.

Great effort has been devoted to investigating the morphology and property of C-A-S-H gel by means of experimental studies and simulation techniques. Experimental results provided significant insights into the structural mechanisms of Al-substitution in the C-S-H phase. NMR test shows some local structure information of Aluminate atoms [9] [10] [11]. The tetrahedral, pentahedral and octahedral aluminate species coexist in the C-A-S-H gel. The multiple roles of Al atoms are due

to the complicated environment of Al species in the C-A-S-H gel: While the Al^{IV} occurs on the bridging tetrahedra of the drierkette Al-silicate chains, and Al^{V} and Al^{VI} occur in the interlayer and perhaps on particle surfaces. In addition, with increasing of Ca/Si ratio for the C-S-H gel, the location of the aluminate species incorporation also varied significantly [12]. It is also worth noting that the aluminate species are coordinated by the highly adsorbed water molecules and hydroxyls [13]. Furthermore, experimental results also demonstrated that aluminate species can enhance polymerization due to their tendency to form bridging tetrahedron between silicate units [14] [15]. By using NMR testing [16] [17], it is widely accepted that C-A-S-H gel has longer silicate chains than that in C-S-H gel in the OPC cement paste. Additionally, the signal of the Q_3 species in the spectrum indicates the network structures appearance [11], which has not been observed in the C-S-H gel.

Based on the findings from experiments, molecular simulation has been utilized to give a more comprehensive understanding for the structure of C-A-S-H gel. Puertasa [16] constructed a model by replacing the silicon with aluminum atom in tobermorite 11 Å and 14 Å (the mineral analogue of the C-S-H gel). Even though the model can predict the mechanical properties of the C-A-S-H gel, the tobermorite structure is not able to represent the real structure of C-S-H gel in respect of the chemical composition and density [18]. Recently, by using empirical force field simulation, the C-A-S-H model has been constructed by substituting the atoms in the "realistic model" of C-S-H with aluminum atoms [19]. This work can be considered as a new application for a realistic model and provides new insights on the local structure, the connectivity of the Q species as well as the deformation of C-A-S-H gel. However, the C-A-S-H gel model should be further improved in two respects: empirical force field cannot describe the dissociation of water molecules so that no hydroxyl is present in the C-A-S-H gel; the Q species distribution in the realistic model overestimates the Q_0 species so that the silicate skeleton role is weakened [20].

In this work, reactive force field molecular simulation is employed to investigate the structural, dynamical and mechanical properties of the C-A-S-H gel. The model of C-A-S-H gel is constructed by replacing the Si atoms and interlayer Ca atoms in the improved "realistic model" of the C-S-H gel. The Si-Al substitution in silicate chains has been widely confirmed by the experimental findings [21]. However, the Ca-Al substitution can be understood as the Al atoms presence in the interlayer region. In this way, the complicated local environment of Al atoms can be investigated. With different substitution ratio of aluminum atoms, the role of aluminum atoms in the structure and dynamic properties can be investigated. Additionally, uniaxial tension test simulates the deformation of the C-A-S-H gel and provides the stiffness and cohesive force in the gel.

2. Method

2.1 Reactive force field

The Reactive force field (ReaxFF), developed by van Duin et al [22], is utilized to simulate the chemical reaction for both atomic structure construction and uniaxial tensile testing. The Reactive force field provides an advanced description of the interaction between Ca, Si, Al, O and H atoms in the C-S-H gel. The short-range interactions for the ReaxFF are determined by a bond length-bond order scheme so that the bonds can be broken and formed, with the potential energy transforming into a smooth state [23]. On the other hand, the long-range coulombic interactions are determined by a 7^{th} order taper function, with an outer cut off radius of 10 Å. The Reactive Force field has been widely utilized in silica-water interfaces [24], calcium silicate hydrate gel [25] and nano-crystals [26]. The parameters of the force field for Ca, Si, Al, O and H can be directly obtained from previous published reference data [22] [27] [28].

2.2 Model construction

For the C-A-S-H gel, the model construction in the present study is based on the procedures that combine the methods proposed by Hou [29], Pellenq [18] ,Manzano [30] and Qomi [19]. Firstly, the layered analogue mineral of C-S-H, tobermorite 11Å without water, was taken as the initial configuration for the C-S-H model [31] [32]. Silicate chains were then broken to match the Q species distribution with Q_1=73.9%, Q_2=21.4% and Q_0=4.7%. The mean silicate chain length (MCL=2(Q_2/Q_1+1)=2.58) is consistent with the results obtained both from NMR testing [33] and molecular dynamics simulation [34]. It is worth noting that the Q_0 percentage is controlled to less than 5%, also matching well with experimental results [35]. Meanwhile, the Ca/Si ratio ranges from 0.7 to 2.3 with an average value of 1.7. In order to increase the Ca/Si ratio, some of the bridging SiO_2 units are first removed as proposed by Pellenq et al. [18]. More importantly, some dimer structures (Si_2O_4) are also removed to satisfy the Q species distribution, especially for low Q_0 percentages. After omission of the dimer structure, to maintain charge neutrality, some oxygen atoms in the silicate chains have to remain in the form of dangling atoms. It should be noted that the dangling atoms are not the final state for the oxygen atoms. After water adsorption and reactive force field MD in the following procedures, the dangling oxygen atoms can react with neighboring water molecules and transform to hydroxyls group. In this way, the dry calcium silicate skeleton is obtained, as shown in Fig.1.

Subsequently, the silicon atoms in the chains and interlayer Ca atoms are gradually replaced by the Al atoms, respectively. Considering the charge balance, the Si-Al substitution requires including some H atoms by transforming Si-O bond to Si-OH. For the Ca-Al substitution, two Al^{3+} atoms replace three Ca^{2+} atoms to maintain the charge neutrality. For the former case, five dry C-A-S-H samples with Al/Si ratio of 0, 0.075, 0.133, 0.3 and 0.88 can be constructed. For the latter case, five dry C-A-S-H samples with Al/Ca ratio of 0, 0.075, 0.16, 0.26 and 0.38 can be obtained (Al/Ca=0 is the C-S-H gel).

After the dry samples were constructed, the Grand Canonical Monte Carlo (GCMC) method was utilized to investigate the structure of the dry calcium aluminate silicate skeleton, immersed in water solution [36]. The dry sample obtained by temperature quenching method is utilized for simulation. GCMC simulations determine the properties of the water molecules confined in the calcium aluminate silicate system at constant volume V in equilibrium with a fictitious infinite reservoir of liquid bulk water solution that imposes its chemical potential μ=0 eV and its temperature T=300 K [18]. The simulation process is analoguous to water adsorption in micro-porous phases such as calcium silicate hydrate and zeolite [37].The simulation included 300,000 circles for the system to reach equilibrium, followed by 100,000 circles for the production run. For each circle, it is attempted to insert, delete, displace and rotate water molecules 1000 times in the constant volume calcium aluminate silica hydrate system.

Finally, the chemical formula of the saturated C-S-H structure in the current simulation is given by $(CaO)_{1.69}(SiO_2)\cdot(H_2O)_{1.82}$, which is quite close to $(CaO)_{1.7}(SiO_2)\cdot 1.8H_2O$ obtained by the SANS test [38]. The reactive force field molecular dynamic simulations under constant pressure and temperature (NPT) for 300 ps give the structures of C-S-H gel at equilibrium states. A further 1000 ps NPT run is employed to achieve the equilibrium configuration for structural and dynamic analysis.

2.3 Uniaxial tension test

Uniaxial tension testing is employed to investigate the mechanical behavior of the tobermorite and the C-S-H gel. Super-cells, obtained by periodically extending the simulated model in section 2.2 by a factor of two, underwent uniaxial tension in the ***y*** and ***z*** direction. The super-cells were composed of 7744 atoms to 8064 atoms, with the size around 40 Å × 40 Å × 40 Å. It should be noted that using a large number of atoms in this study can give stable statistical simulation results, especially in regard to

reliable failure modes. In order to explore the failure mechanism of the layered structure, the stress-strain relation and the deformation of the molecular structure were investigated in the loading process.

To obtain the stress-strain relation, the structure was subjected to uniaxial tensile loading through gradual elongation at constant strain rates of 0.08/ps. In the whole simulation process, NPT ensembles are defined for the system. Take the tension along ***y*** direction for example. Firstly, the super-cells were relaxed at 300K and coupled to zero external pressure in the ***x***, ***y***, ***z*** dimensions for 500 ps. Then, after the pressures in the three directions reached equilibrium, the C-S-H structure would be elongated in the ***y*** direction. Meanwhile, the pressure in ***x***, ***z*** direction was kept at zero. Pressure evolution in the ***x*** direction was taken as the internal stress σ_{yy}. Setting the pressure perpendicular to the tension direction to zero can allow the normal direction to relax un-isotropically without any restriction. The setting, considering Poisson's ratio, can eliminate the artificial constraint for the deformation.

3. Results and discussion

For the samples with Si-Al substitution, the simulated molecular structure of C-A-S-H at the Al/Si ratio of 0.075 is shown in Fig.2a. It shows that the incorporation of aluminate atoms has not changed the silicate skeleton in great extent. The aluminate atoms present in the bridging and pairing site of the chains grows along y directions. No further polymerization and de-polymerization can be observed in the silicate-aluminate chains, indicating the chemical stability of the Al-Si substitution. The Si substitution for Al is possible due the similar size and charge of these atoms. This matches well with NMR findings that the Al substitution is in the silicate chains in many synthesized C-S-H gels [10] [11]. In addition, five-coordinated aluminate species are widely found in the aluminate silicate chains. The aluminate atoms, closed to the interlayer water molecules and hydroxyl groups, are probable to have a strong Al-O_w connection.

On the other hand, for the aluminate atoms presence in the interlayer region, the molecular structure of C-A-S-H gel has been changed significantly. The simulated molecular structure of C-A-S-H at an Al/Ca ratio of 0.075 is shown in Fig.2b ; Correspondingly, the intensity profiles of different atoms at equilibrium state are plotted in Fig.2c versus the distance in the ***z*** direction. It can be clearly observed in Fig.2b that calcium atoms and the surrounding oxygen atoms form a Ca-O octahedral, constructing the Ca sheet. Defective silicate chains graft on both side of the Ca sheets in the C-S-H gels. Between the neighboring calcium silicate sheets located the interlayer calcium atoms (Ca_w), aluminum atoms and water molecules. As shown in Fig.2c, the alternative maxima of Ca, Si, Al and H atoms in the density profiles indicate that C-A-S-H gel has a sandwich-like structure. In the intra-layer, Al atoms grow into the deficient region of the broken silicate chains and elongate the silicate chain length in ***y*** direction. Besides, the healing effect of the Al atoms in molecular structure reconstruction can enhance the interlayer connections. As shown in Fig.2d, Al atoms are distributed continuously across the interlayer region, with increasing Al content. It is valuable to note that the Al atoms, associated with the non-bridging oxygen atoms in the defective silicate chains, bridge the neighboring calcium silicate sheets. In this way, the aluminum-silicate network is gradually constructed in the interlayer region. Hence, the addition of Al atoms can transform the C-S-H gel from a layered crystal to a glassy-like structure.

On the other hand, irregular distribution of the H atoms in the interlayer region implies that the structure of the water molecules, highly confined by the nano pores, is significantly distorted by the complicated local calcium aluminate silicate environment. The large intensity peaks of the H atoms also reflect that the defective silicate chains, with large numbers of NBO atoms, have good ability to adsorb water molecules. In Fig.2b, the intensity distributions of the H atoms and Si atoms overlap, which means that water molecules not only are present in the interlayer regions but also diffuse into the defective region of the calcium silicate sheet. Additionally, the

aluminate hydroxyls observed in the interlayer region, imply that the addition of Al atoms has great influence on the hydrolytic reaction of the water molecules.

In order to give more quantitative insights on the molecular structure of C-A-S-H gel, the local structure of the Al atoms is further investigated by the Q species distribution, the radial distribution function, the angle distribution function and the coordination number.

3.1 Connectivity factor

As in the silicate composite structure, the connectivity factor, Q_n (n=0, 1, 2, 3, 4) is an important parameter to estimate the silicate connection, where n is defined as the number of connected neighboring silicate tetrahedrons. Q_0 is the monomer; Q_1 represents the dimer structure (two connected silicate tetrahedrons); Q_2 is the long chain; Q_3 is the branch structure; Q_4 is the network structure (Feuston and Garofalini, 1990). For the aluminate-silicate substitution, the Q species distribution maintains unchanged. At Ca/(Al+Si) ratio of 1.7, the dimer structure have predominant percentage. On the other hand, the aluminate species in the interlayer region change the Q species distribution significantly. As shown in Fig.3a, with a decreasing Ca/(Al+Si) ratio from 1.7 to 0.9, the percentage of Q_1 species is reduced significantly from around 74% to 20%. The Q_0 species completely disappeared, when the Ca/(Al+Si) ratio reached 0.9. On the contrary, the ratios of Q_2, Q_3 and Q_4 species grew to 51.6%, 17.9 % and 7.4%, respectively. It is worth noting that the growth of the Q species follows the sequence: Q_2, Q_3 and Q_4. This trend indicates that the silicate-aluminate structures first transform from the short dimer structure to long chains at low aluminum content, and subsequently turn to branches and network structures at high aluminum content. The Q species distribution in the current simulation confirms the observation by NMR experiment that the signal of Q_2 species is intensified and Q_3 species is appeared [11]. The mean chain length, defined as

$MCL = 2(\frac{Q_2}{Q_1} + 1)$, is calculated as a function of the Ca/(Al+Si) ratio. As shown in Fig. 3b, the tendency that MCL decreases with increasing Ca/(Al+Si) ratio matches well with the results obtained from previous simulation by the empirical force field method [19] and experimental work by NMR [16] [39]. Additionally, as shown in Fig.3c, the percentage of Q_2, Q_3 and Q_4 species, reflecting the polymerization degree, reduces with increasing Ca/(Si+Al) ratio. However, compared with the percentages obtained from previous simulations by the empirical force field method [19], the current simulation work demonstrates higher values. In particular, at a Ca/(Si+Al) ratio around 1.2, the percentage of Q_3 and Q_4 species is 16%, twice as large as the value from previous simulations. The large discrepancy reflects different polymerization mechanisms predicted by the reactive force field and the empirical force field.

The connectivity transition is attributed to the polymerization role of the aluminum atoms in the network construction. On the one hand, as shown in Fig.3d, the Al atoms connect with the NBO atoms in the defective silicate chains so the long aluminate-silicate chain is formed. Since the number of NBO atoms coordinated with the Al atom ranges from 1 to 4, the aluminate structure varies from Q_1 to Q_4. This reaction between Al and silicate chains can both be described by the reactive and empirical force fields. On the other hand, when the NBO sites in the silicate chains are occupied by the Al atoms at high Al/Ca ratios, polymerization reaction between different Al species occurs. Fig.3e shows the reaction process: one water molecule diffuses to one nearby Al atom and forms a Al-O_w (O_w: oxygen atom in water) connection; subsequently another Al-O_w bond is also constructed; finally water dissociate one hydrogen atom and stable Al-O_h-Al bond is formed (O_h: oxygen atom in hydroxyl). Water molecules play an essential role in bridging the two neighboring Al species during the polymerization process. Meanwhile, the O_w atoms transform to the bridging oxygen atoms (BO) in the aluminate-silicate skeleton. Since the empirical force field can only simulate Al-O_w rather than further water dissociation process, the Q_3 species formation is restricted to a great extent.

3.2 Local structure of Al atoms

RDF curves of Al-O bonds in C-A-S-H gel with different Al/Ca ratios are plotted in Fig.4a. For bonded atoms, the relevant bond distances can be readily determined by the positions of the peaks in the corresponding RDF. In the C-A-S-H gels, the reactive force field yielded a Al-O bond distance from 1.88 Å to 1.89Å, which is close to the value of 1.9 Å obtained from previous simulations involving in the empirical force field [19]. In the medium range, the Al-O spatial correlation in C-A-S-H is extended to 4 Å, at which point the intensity peaks gradually increase with Al concentration. The longer distance correlation in the C-A-S-H gel at high Al/Ca ratios can be interpreted as a stronger connection attributed to the branch structure formation.

For the Al-Si substitution, as shown in Fig.4b, the coordinated number (CN) of aluminum atoms, describing the amount of the neighboring oxygen atoms, ranges from 4 to 6 , with 4 occupying predominant percentage. It means that the aluminate species in the silicate chains are mainly in form of tetrahedrons. On the other hand, as shown in Fig.4c, the CN distribution indicates that the structures of aluminate atoms are pentahedrons and octahedrons. It should be noted that in NMR testing, the relative concentration of visible Al^{V} and Al^{VI} species account for 85% of the hydrated aluminate cement products, with 15% Al^{IV} species [9]. In addition to confirm coexistence of Al^{IV} Al^{V} and Al^{VI} species in the C-A-S-H gel, the simulation results also suggest that the aluminate species located in calcium silicate sheet and interlayer region demonstrate different local structures.

In previous experiments [9], 2D $^{29}Si\{^{1}H\}$ and $^{27}Al\{^{1}H\}$ NMR spectra revealed that heterogeneous distributions of hydroxyl species and strongly adsorbed water are present in the hydrated aluminate products. MD simulation can quantitatively access those hydroxyl and water molecules associated with Al atoms. As shown in Fig.4d, the coordinated oxygen atoms of the Al species are decomposed into hydroxyl oxygen

(O_h), bridging oxygen (O_b) and water oxygen (O_w) to analyze the local structural difference. The hydroxyl groups in the C-A-S-H gel are produced by the hydrolytic reaction. The water molecules dissociate into H^+ and OH^- ionic pairs; the former diffuse near the O_{NB} sites in the defective silicate chain, forming silicate hydroxyl. The remaining OH^- group can either associate with Ca_w atoms or Al atoms in the interlayer region. It is interestingly noted that O_b in the Al-O_b-Al and Si-O_b-Al can further react with water, forming an O_b-H bond. This is quite different to the siloxane bond (Si-O-Si) in the C-S-H gel in that the O_b atoms have no any reactivity with water molecules [30]. The reactivity discrepancy indicates that the Al-O-Al bond has a hydrophilic feature, contrary to the hydrophobic nature of bridging oxygen atoms in the siloxane bond. Fundamentally, electronic attraction of Al-O_b is slight weaker than that of Si-O_b, which prevents additional H^+ from associating.

Table 1 lists the average coordination number (CN) of aluminate atoms at different Al/Ca ratios. In all the C-A-S-H gels, the CN value of O_b and O_h atoms is more than 4.6, which is more than 85% of the total CN. The small ratio of coordinated O_w atoms implies that the water molecules strongly absorbed by the Al atoms probably dissociate into hydroxyl and H^+. Besides, as shown in Table.1, with increasing Al/Ca ratios, the reduction of the CN value for O_h is accompanied by the increase of O_b. The transition from O_h atoms to O_b atoms is attributed to the polymerization of the aluminate species, as discussed in the previous section.

Table.1. Average coordination number per Al atom in the C-A-S-H with different Al/Ca ratio. Coordinated oxygen atoms include O_h, O_b and O_w

Al/Ca	O_h	O_b	O_w	Total
0.075	2.3	2.5	0.6	5.4
0.16	2.05	2.55	0.7	5.3
0.26	2.03	2.63	0.8	5.47
0.38	1.8	3	0.6	5.4

The O-Al-O angle distribution, exhibited in Fig. 4e, provides geometric information on the aluminum-oxide local structure. The angle distribution for C-A-S-H is characterized by one intense and narrow peak at around 80°, and a small and broad peak at 160°, that correspond to the distorted Al-O octahedral or pentahedral arrangement. It should be noted that the peak at 80° has also been observed in calcium aluminate glass [40] and silicate-aluminate glass [41] at high aluminum concentration, implying an amorphous glassy nature for the local structure of the Al atoms. Besides, as shown in Fig.4e, a shoulder located at around 90° for the C-A-S-H gel gradually disappears with increasing Al/Ca ratio and the second peak at 160° become more pronounced at high Al/Ca ratios. The angle distribution evolution reflects the interaction between aluminate species and silicate chains at different Al/Ca ratios. At low Al/Ca ratio, the defective silicate chains provide a large amount of NBO sites for the Al-O bond to restrict the geometric arrangement for aluminate octahedral. Since 109° is a typical value for the silicate tetrahedron structure, the aluminate octahedron is significantly influenced, resulting in a large shoulder in the angle distribution. On the other hand, at high Al/Ca ratio, the interplay between neighboring aluminate species dominates the angle distribution, which weakens the silicate chains' effect. Apart from the influence of the defective silicate chains, the highly solvated calcium atoms confined in the interlayer region and the two dimensional confined geometry of the layered structure all determine the distorted octahedral structure of the aluminate species.

3.3 Dynamic properties

The previous discussion describes the molecular structure of C-A-S-H gel at different Al/Ca ratios. The chemical bonds of Si-O, Ca-O, Al-O, H-O and the H-bonds play roles in bridging the neighboring calcium silicate sheets. The strengths of the bonds depend on the stability of the chemical bonds to a large extent. As in previous research studying the H-bonds strength [42], the time correlated function (TCF) is utilized to describe the dynamical properties of various chemical bonds.

TCF C(t) of a bond is described in Eq (1):

$$C(t) = \frac{<\delta b(t)\delta b(0)>}{<\delta b(0)\delta b(0)>} \quad (1)$$

where $\delta b(t) = b(t) - < b >$, b(t) is a binary operator that takes a value of one if the pair (e.g. Ca-O) is bonded and zero if not, and <b> is the average value of b over all simulation times and pairs. The chemical bonds break and form during the time evolution, which result in the connectivity variation in C-A-S-H gels. If the connectivity persists unchanged, the TCF of the bonds will maintain a constant value of one. Otherwise, the breaking of the bonds leads to lower TCF values, and the more frequent the bond breakage, the lower the value of TCF. By comparing the deviations from one in the TCF curves, the stability of the various bonds can be estimated.

Fig.5a demonstrates the evolution of the TCFs of Si-O, Ca-O, Al-O, H-O and H-bonds of C-A-S-H at an Al/Ca ratio of 0.26 in 10 ps during the equilibrium state. According to the reduction extent of *C(t)*, the strength of the chemical bonds is ranked in the following order: Al-O, Si-O > O-H, Ca-O > H-bonds. The *C(t)* value of Si-O and Al-O almost remains at one without any reduction with time. It implies that silicate-aluminate network, having good stability, acts as the skeleton of the C-A-S-H gel.

On the other hand, the slight reduction of *C(t)* for O-H bond and Ca-O bond indicates a weaker connection than the silicate-aluminate skeleton. Water molecules and hydroxyl groups continuously dissociate and associate to maintain the hydrolytic equilibrium. The variation for the Ca-O bonds is mainly attributed to the frequent breakage of the connection between the water molecules and the interlayer Ca atoms. Ca_w atoms form clusters with water in the interlayer region, and the diffusion rate is thus accelerated to some extent. In respect of the chemical bonds, substitution of the

interlayer Ca atoms with Al atoms transforms unstable Ca-O_w bonds to the high strength Al-O skeleton, which improves the stability of the interlayer region.

The lowest C(t) value of the H-bonds is partly attributed to the high diffusion rate of water molecules and is partly caused by the water reaction with neighboring Ca_w atoms and Al atoms. Hence, the stability of H-bonds depends greatly on the local environment in the interlayer region. As shown in Fig.5b, the *C(t)* value for H-bonds gradually increase, as Al/Ca ratio becomes higher. Since O_w atoms in the water molecules transform to the O_h and O_B atoms due to the polymerization role of Al atoms, the percentage of H-bonds accepted by the structural oxygen atoms increases significantly. According to H-bond strength analysis by Youssef [42], the H-bonds formed by neighboring water molecules have lower strength than those constructed between structural oxygen and water molecules. Therefore, the H-bonds stability is indirectly enhanced due to the addition of Al atoms. The dynamic properties of the Si-O bonds, Al-O bonds and Ca-O bonds match well with previous findings by ab initio method [43] [28]. The findings prove that Si-O bonds, Al-O bonds in the calcium silicate aluminate minerals have more binding energy than Ca-O bonds and are hard to break.

3.4 Stress-Strain relation

The stress-strain curve can characterize the mechanical behavior of a layered structure during the tensile process and help gain insights into the constitutive relation between stress and strain. Different stress-strain relations of tensile loading in the ***y*** and ***z*** directions indicate the heterogeneous nature of layered structures. In the ***y*** direction, as shown in Fig.6a, during the tensile process, stress first increases linearly in the elastic stage and subsequently slowly increases to a maximum of 6.5 GPa at a strain around 0.17 Å/Å. After the maximum, the stress directly reduces slowly without obvious yield behavior. Even at strain 0.8 Å/Å, the stress does not drop to zero,

implying good plasticity along the ***y*** direction. On the other hand, the C-S-H gel is more likely to suffer breakage in the ***z*** direction, with the strain at the fracture state 0.4 Å/Å, indicating that the interlayer structure shows more brittle features. The mechanical performance discrepancy in different directions confirms that the ionic-covalent bonds in the calcium silicate sheet are quite stronger than the H-bonds' strength in tensile loading resistance.

For the Si-Al substitution, as shown in Fig.6c, in the y direction, the stress-strain curves of C-A-S-H resemble that of C-S-H. The Young's modulus and the tensile strength have not been changed in great extent. It can be explained by the structural and dynamical role of Al atoms in the silicate chains. On one hand, the Si-Al substitution has not improved the polymerization degree in the silicate skeleton. In the respect of the bond stability, as discussed in previous section, the Al-O and Si-O bond demonstrate equivalent bond strength. Hence, mechanical performance is not improved due to the Si-Al substitution.

On the contrary, for the Ca-Al substitution, as shown in Fig. 6d and e, with progressively increasing Al/Ca ratio from 0 to 0.38, Young's modulus grows from 64 GPa to 75 GPa along the ***y*** direction and from 50 to 68 GPa along the ***z*** direction. The stiffness improvement is greatly related to the polymerization changes for the C-S-H gel with Al addition, as discussed in the connectivity section. Al species play a critical role in connecting the defective silicate chains and in transforming C-S-H gel from the layered structure to a 3 dimensional network. While E_y increases significantly as the Al/Ca ratio is less than 0.2, the pronounced enhancement for E_z is from Al/Ca 0.26 to 0.38. The moduli evolution trend reflects the growth order for the aluminate network: at low Al/Ca ratios, the Al atoms mainly heal the defective calcium silicate sheet; at high Al/Ca ratios, the branches are constructed in the interlayer region. Young's moduli obtained in current simulations are consistent with the results from nano-indentation testing (60 GPa) [44], previous ab initio calculations (55 Gpa ~68 Gpa) [18] and molecular mechanical calculation (56~61.6 GPa).

Similar evolution trends in the tensile strength can be observed in Fig.6f and Fig.6g. The tensile strength increases from 6.5 GPa of C-S-H gel to 8.5 GPa of C-A-S-H gel with Al/Ca 0.38 in the ***y*** direction and from 3.25 GPa to 7 GPa in the ***z*** direction. The failure stresses obtained here are consistent with the rupture strength (~3 GPa) by shear simulation [18] and fluid pressure (2.75 GPa) calculation [36]. The huge strength discrepancy between C-S-H gel and C-A-S-H gel indicates different failure mechanisms. The chemical bonds determine the mechanical performance in different Al concentrations to a large extent. When Ca_w atoms are substituted by Al atoms, the unstable Ca-O_w bonds and H-bonds are partially substituted by the stable and high strength Al-O_b bonds, while the structure transforms from a layered structure to a network structure. The variations of the chemical bonds and structure that play important roles in bridging the calcium silicate sheets result in the strengthening of the cohesive force. In the aspect of "hydrolytic weakening", Bonnaud proposed the disjoining effect of water molecules in C-S-H grains [36] in which the fluid pressure in the C-S-H gel is contributed by the repulsive force by the water molecules. However, in the C-A-S-H gel, water molecules, absorbed by the Al atoms, are further dissociated and transformed to bridging oxygen atoms or the hydroxyls that are connected firmly with the calcium-aluminate-silicate structure. Hence, there is less chance for the water molecules to attack the ionic-covalent bonds.

3.5 Deformation of the structure

More information can be obtained from examining the deformed molecular structure of the C-A-S-H gel and C-S-H gel in resisting tensile loading. As shown in Fig.7b, Ca-O bond breakage can be widely observed in the damaged C-S-H gel. Since the short silicate chains are separately distributed in the calcium silicate sheet, the mechanical contribution for the silicate chain, such as the siloxane bond stretching and the enlargement of the Si-O-Si angle, is limited to a great extent. On the contrary, in the C-A-S-H gel, the Al atoms heal the defective silicate chains and construct a

relatively integral network structure. Hence, the changes of the Si-O-Al bonds and angles carry a major percentage of the tensile loading. It can be observed in Fig.7a that the breakage of Si-O or Al-O bonds results in the de-polymerization of the aluminate-silicate network during the tensile process.

To quantitatively access the morphology variation, the Q species distribution is monitored as a function of the strain. As shown in Fig.7c, the percentages of the Q_0, Q_1 and Q_2 species maintain constant values, implying that the short silicate chains are hard to be stretched broken. On the other hand, as shown in Fig.7d, the Q_2 species continuously decrease from 52.5% to 45%, while the Q_1 species increase from less than 20% to 25%. Additionally, the total variation of Q_0, Q_3 and Q_4 species is less than 2.5%. The transformation from Q_2 to Q_1 species implies that the long silicate chain is stretch broken into short silicate chains. Meanwhile, the newly formed short chains can be reconstructed with the neighboring aluminate-silicate network, which contributes to a small amount of other Q species. In this respect, the structural evolution due to tensile stretching can be interpreted as the de-polymerization of the silicate-aluminate network. The aluminate branches (Q_3 and Q_4) species, strongly restricted by the Al-O and Si-O bonds, can give great mechanical contribution by local structural rearrangement. By previous ab initio calculation [43], the presence of the Q_3 species can improve the interlayer connection of tobermorite [45](a kind of calcium silicate crystal) by forming a hinge mechanism.

Furthermore, as shown in Fig. 7a and Fig. 7b, in both deformed C-S-H gel and C-A-S-H gel, the broken calcium silicate aluminate bonds are terminated by forming hydroxyl. As shown in Fig. 7e, the number of Si-OH and Al-OH bonds continuously increase during the tensile process, implying a progressive dissociation of water molecules. The mechanism of the hydrolytic reaction is that the tensile loading results in local bonds elongation or even breakage, which lowers the energy barrier for the water dissociation [46] [47]. As compared with BO sites, water molecules are more likely to react with the NBO sites in aluminate-silicate chains. It also should be noted

that at higher Al/Ca ratios, the hydroxyl number have a larger value in Fig. 7e. Since the de-polymerization reaction widely occurs at high Al/Ca ratios, more BO sites in the aluminate-silicate chains transform to NBO sites. In this way, water dissociation, accompanied by aluminate-silicate de-polymerization, produces large amounts of hydroxyl bonds.

4. Conclusions

Reactive force field molecular dynamic simulation was employed to investigate the molecular characteristics of the C-A-S-H gel, including the structural, dynamical and mechanical properties. Following conclusions can be made from this work.

1）The Si-Al substitution in the calcium silicate sheet has not changed the layered structure of C-A-S-H gel. On the other hand, the Al atoms, presence in the interlayer region, improve the structure and mechanical performance significantly.

2) The Q species evolution trend indicates that the silicate-aluminate structures first transforms from the short dimer structure to the long chains at low aluminum content and subsequently turn to branches and network structures at high aluminum content.

3) The structural transition is partly attributed to the aluminate-silicate connection by the NBO sites and is partly caused by the polymerization reaction between the aluminate species, both of which can be described by the Reactive Force Field.

4) The coordinated oxygen atoms of aluminum atoms include water, hydroxyl and bridging oxygen atoms. Due to the polymerization reaction, partial hydroxyl groups transform to the bridging oxygen atoms.

5) Dynamically, due to the strong strength of the Al-O bond, the aluminate-silicate network in C-A-S-H gel has better stability at higher Al/Ca ratios. The stable aluminate species also strengthens the neighboring H-bonds network significantly.

6) Uniaxial tension testing, performed on C-A-S-H gels, demonstrate the mechanical behavior and large structural deformation of the gel. Both Young's modulus and the tensile strength are improved significantly with increasing aluminum content, indicating the good loading resistance ability of aluminate-silicate networks.

7) Tensile deformation, simulated by the reactive force field, is also coupled with the de-polymerization of aluminate species and the water dissociation reaction, which shows good plasticity due to the addition of Al atoms.

Acknowledgement

Financially support from the China Ministry of Science and Technology under Grant 2015CB655100 and Major International Joint Research Project under Grant 51420105015 are gratefully acknowledged.

Reference

[1] Z. Li, Advanced Concrete Technology, Hoboken, N.J.: John Wiley & Sons Inc, 2011.

[2] A. Scott and M. Thomas, "Evaluation of Fly Ash From Co-Combustion of Coal and Petroleum Coke for Use in Concrete," *ACI Materials Journal ,* vol. 104 , no. 1, p. 62–70., 2007.

[3] C. Hu and Z. Li, "Micromechanical investigation of Portland cement paste," *Construction and Building Materials,* vol. 71, pp. 44-52, 2014.

[4] I. Richardson, "The nature of calcium silicate hydrate," *Cement and Concrete Research, 29,* pp. 1131-1147, 1999.

[5] H. Ma, D. Hou, J. Liu and Z. Li, "Estimate the relative electrical conductivity of C–S–H gel from experimental results," *Construction and Building Materials,* vol. 71, pp. 392-396, 2014.

[6] L. Zhang, Z. Lin and Z. Li, "The structure of silicate ions in CSH discussed from chemical composition," *Advances in Cement Research,* vol. 24, no. 5, pp. 263-281, 2012.

[7] A. Emwas, P. Monteiro, M. Jackson, S. Chae, S. Mulcahy, C. Meral, R. Taylor, P. Li, J. Moon, G. Vola and H.-R. Wenk, "Unlocking the secrets of Al-tobermorite in Roman seawater concrete," *American Mineralogist,* vol. 98, pp. 1669-1687, 2013.

[8] M. D. Jackson, J. Moon, E. Gotti, R. Taylor, S. R. Chae, M. Kunz, A.-H. Emwas, C. Meral, P. Guttmann, P. Levitz, H.-R. Wenk and P. J. M. Monteiro, "Material and Elastic Properties of Al-Tobermorite in Ancient Roman Seawater Concrete," *Journal of the American Ceramic*

Society, vol. 96, pp. 2598-2606, 2013.

[9] A. Rawal, B. Smith, G. Athens, C. Edwards, L. Roberts, V. Gupta and B. Chmelka, "Molecular Silicate and Aluminate Species in Anhydrous and Hydrated Cements," *Journal of American Chemistry Society,* vol. 132, no. 21, p. 7321–37, 2010.

[10] M. D. Andersen, H. J. Jakobsen and J. Skibsted, " Incorporation of aluminum in the calcium silicate hydrate (CSH) of hydrated Portland cements: A high-field 27Al and 29Si MAS NMR investigation," *Inorganic chemistry,* vol. 42, no. 7, pp. 2280-2287, 2003.

[11] G. Sun, J. Young and R. Kirkpatrick, "The Role of Al in C-S-H: NMR, XRD, and Compositional Results for Precipitated Samples," *Cement and Concrete Research,* vol. 36, no. 1, pp. 18-29, 2006.

[12] P. Faucon, A. Delagrave, J. C. Petit, C. Richet, J. M. Marchand and H. Zanni, "Aluminum incorporation in calcium silicate hydrates (CSH) depending on their Ca/Si ratio," *The Journal of Physical Chemistry B,* vol. 103, no. 37, pp. 7796-7802, 1999.

[13] M. Andersen, H. Jakobsen and J. Skibsted, "A new aluminium-hydrate species in hydrated Portland cements characterized by 27Al and 29Si MAS NMR spectroscopy," *Cement and Concrete Research,* vol. 36, no. 1, pp. 3-17, 205.

[14] S. Komarneni, R. Roy, D. Roy, C. Fyfe, G. Kennedy, A. Bothner-By, J. Dadok and A. Chesnic, "27Al and 29Si magic angle spinning nuclear magnetic resonance spectroscopy of Al-substituted tobermorites," *Journal of Material Science (1985) ,* vol. 20, p. 4209–4214, 1985.

[15] M. Tsuji, S. Komarneni and P. Malla, "Substituted tobermorites: 27Al and 29Si MAS NMR cation exchange, and water sorption studies," *Journal of American Ceramic Society,* vol. 74, pp. 274-279, 1991.

[16] F. Puertas, M. Palacios, H. Manzano, J. S. Dolado, A. Rico and J. Rodríguez, "A model for the C-A-S-H gel formed in alkali-activated slag cements," *Journal of the European Ceramic Society,* vol. 31, no. 12, p. 2043–2056, 2011.

[17] R. Taylor, I. Richardson and R. Brydson, "Composition and microstructure of 20-year-old ordinary Portland cement–ground granulated blast-furnace slag blends containing 0 to 100% slag," *Cement and Concrete Research,* vol. 40, no. 7, pp. 971-983, 2010.

[18] R. J. Pellenq, A. Kushima, R. Shahsavari, K. J. Van Vliet, M. J. Buehler and S. Yip, "A realistic molecular model of cement hydrates," *PNAS,* vol. 106, no. 38, p. 16102–16107, 2009.

[19] M. Qomi, F. Ulm and R. Pellenq, "Evidence on the Dual Nature of Aluminum in the Calcium-Silicate-Hydrates Based on Atomistic Simulations," *Journal of the American Ceramic Society,* vol. 95, no. 3, pp. 1128-1137, 2012.

[20] I. Richardson, "The importance of proper crystal-chemical and geometrical reasoning demonstrated using layered single and double hydroxides," *Acta Crystallographica Section B,* vol. 69, pp. 150-162, 2013.

[21] P. Faucon, J. C. Petit, T. Charpentier, J. F. Jacquinot and F. Adenot, "Silicon substitution for aluminum in calcium silicate hydrates," *Journal of the American Ceramic Society,* vol. 82, no. 5, pp. 1307-1312, 1999.

[22] A. van Duin, A. Strachan, S. Stewman, Q. Zhang, X. Xu and W. Goddard, "ReaxFFsio Reactive Force Field for Silicon and Silicon Oxide Systems," *The Journal of Physical Chemistry A,* vol. 107, no. 19, pp. 3803-3811, 2003.

[23] D. W. Brenner, O. A. Shenderova, J. A. Harrison, S. J. Stuart, B. Ni and S. B. Sinnott, "A second-generation reactive empirical bond order (REBO) potential energy expression for hydrocarbons," *Journal of Physics: Condensed Matt,* vol. 14, no. 4, pp. 783-802, 2002.

[24] S. Leroch and M. Wendland, "Simulation of Forces between Humid Amorphous Silica Surfaces: A comparison of empirical atomic force fields," *The Journal of Physical Chemistry C,* vol. 116, pp. 26247-26261, 2012.

[25] H. Manzano, E. Masoero, I. Arbeloa and H. Jennings, "Molecular modelling of shear deformations in ordered and disordered Calcium Silicate Hydrates," *Soft matter,* vol. 9, no. 30, pp. 7333-7341, 2013.

[26] T. Lau, A. Kushima and S. Yip, "Atomistic Simulation of Creep in a Nanocrystal," *Physical Review Letters,* vol. 104, no. 17, p. 175501, 2010.

[27] H. Manzano, R. Pellenq, F. Ulm and M. Buehler, "Hydration of Calcium Oxide Surface Predicted by Reactive Force Field Molecular Dynamics," *Langmuir,* vol. 28, pp. 4187-4197, 2012.

[28] L. Liu, A. Botero, W. Goddard and H. Sun, "Development of a ReaxFF Reactive Force Field for Ettringite and Study of its Mechanical Failure Modes from Reactive Dynamics simulations," *The Journal of Physical Chemistry A,* vol. 116, pp. 3918-3925, 2012.

[29] D. Hou, H. Ma, Y. Zhu and Z. Li, "Calcium silicate hydrate from dry to saturated state: Structure, dynamics and mechanical properties," *Acta Materialia,* vol. 67, pp. 81-94, 2014.

[30] H. Manzano, S. Moeini, F. Marinelli, A. van Duin, F. Ulm and R. Pellenq, "Confined Water Dissociation in Microporous Defective Silicates:Mechanism, Dipole Distribution, and Impact on Substrate Properties," *Journal of the American Chemistry Society,* vol. 134, no. 4, p. 2208−2215, 2011.

[31] S. J. Murray, V. J. Subramani, R. P. Selvam and K. D. Hall, "Molecular Dynamics to Understand the Mechanical Behavior of cement Paste," *Journal of the transportation Research Board,* vol. 2142, no. 11, pp. 75-82, 2010.

[32] R. P. Selvam, V. G. Subramani, S. Murray and K. Hall, "Potential Application of Nanotechnology on Cement Based materials," 2009.

[33] X. Cong and R. Kirkpatrick, "29Si MAS NMR study of the structure of calcium silicate hydrate," *Advanced Cement Based Material,* vol. 3, no. 3-4, pp. 144-156, 1996.

[34] J. S. Dolado, M. Griebel and J. Hamaekers, "A Molecular Dynamic Study of Cementitious Calcium Silicate Hydrate (C-S-H) gels," *Journal of American Ceramic Society, 90,* pp. 3938-3942, 2007.

[35] A. Brough, C. Dobson, I. Richardson and G. Groves, "In situ solid-state NMR studies of Ca3SiO5: hydration at room temperature and at elevated temperatures using 29Si enrichment," *Journal of Materials Science ,* vol. 29, no. 15, pp. 3926-3940, 1994.

[36] P. A. Bonnaud, Q. Ji, B. Coasne, R. J.-M. Pellenq and K. J. Van Vliet, "Thermodynamics of Water Confined in Porous Calcium-Silicate-Hydrates," *Langmuir,* vol. 28, no. 31, p.

11422−11432, 2012.

[37] J. Puibasset and R. Pellenq, "Grand Canonical Monte Carlo Simulation Study of Water Adsorption in Silicalite at 300 K," *The Physical and Chemistry B,* vol. 112, no. 20, pp. 6390-6397, 2008.

[38] A. J. Allen, J. J. Thomas and H. M. Jennings, "Composition and density of nanoscale calcium silicate hydrate in cement," *Nature material,* vol. 6, pp. 311-316, 2007.

[39] I. Richardson and G. Groves, "The Structure of the Calcium Silicate Hydrate Phases Present in Hardened Pastes of White Portland Cement Blast-Furnace Slag Blends," *Journal of Materials Science ,* vol. 32, no. 18, pp. 4793-802, 1997.

[40] E. Kang, S. Lee and A. Hannon, "Molecular dynamics simulations of calcium aluminate glasses," *Journal of Non-Crystalline Solids,* vol. 352 , p. 725–736, 2006.

[41] A. Winkler, J. Horbach, W. Kob and K. Binder, "Structure and diffusion in amorphous aluminum silicate: A molecular dynamics computer simulation," *The Journal of Chemical Physics ,* vol. 120, no. 1, pp. 384-393, 2004.

[42] M. Youssef, R. J. M. Pellenq and B. Yildiz, "Glassy Nature of Water in an Ultraconfining Disordered Material:The Case of Calcium silicate hydrate," *Journal of American Chemistry Society ,* vol. 133, no. 8, p. 2499–2510, 2011.

[43] R. Shahsavari, M. J. Buechler, R. J. M. Pellenq and F. J. Ulm, "First-principles study of elastic constants and interlayer interactions of complex hydrated oxides: case study of tobermorite and jennite," *Journal of American Ceramic Society, 92,* vol. 92, no. 10, pp. 2323-2330, 2009.

[44] G. Costantinide and F. Ulm, "The nanogranular nature of C-S-H," *Journal of Mechanics and Physics of Solids,* vol. 55, no. 1, pp. 64-90, 2006.

[45] S. Merlino, E. Bonnacorsi and T. Armbruster, "The real structure of tobermorite 11 A: normal and anomalous forms, OD character and polyptic modifications," *European Journal of Mineralogy,* vol. 13, no. 3, pp. 577-590, 2001.

[46] D. Hou, H. Ma, Z. Li and Z. Jin, "Molecular simulation of “hydrolytic weakening”: A case study on silica," *Acta Materialia,* vol. 80, pp. 264-277, 2014.

[47] T. Zhu, J. Li, X. Lin and S. Yip, "Stress-dependent molecular pathways of silica-water reaction," *Journal of Mechanics and Physics of solids,* vol. 53, no. 7, pp. 1597-1623, 2005.

Figure captions

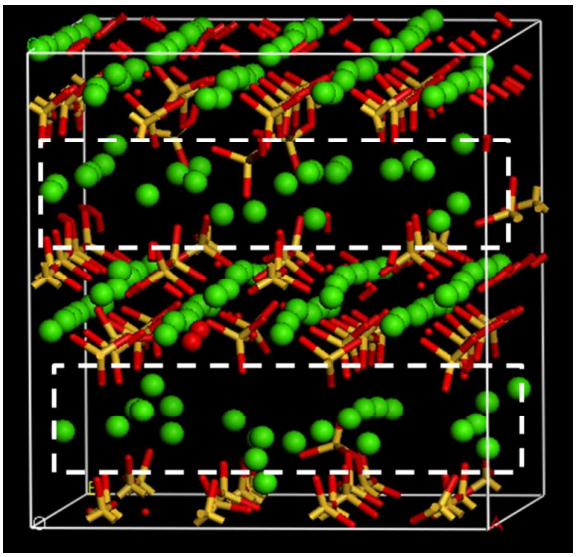

Fig.1. Initial dry C-S-H structure for water adsorption simulation. Simulation box size: ***a***=21.3, ***b***=21.2, ***c***=21.9; ***α***=90°, ***β***=90°, ***γ***=90°. Yellow and red bonds represent the silicate chain (Si-O); the green balls correspond to the calcium atoms and the white red sticks are water molecules. The green balls in the dashed rectangle are the interlayer Ca atoms.

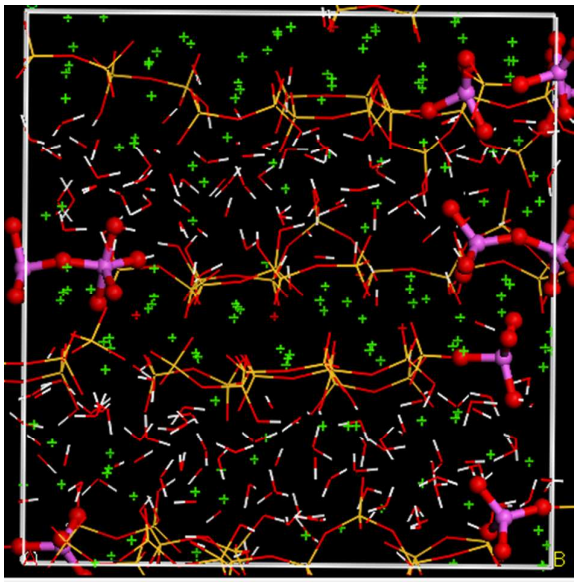

(a)

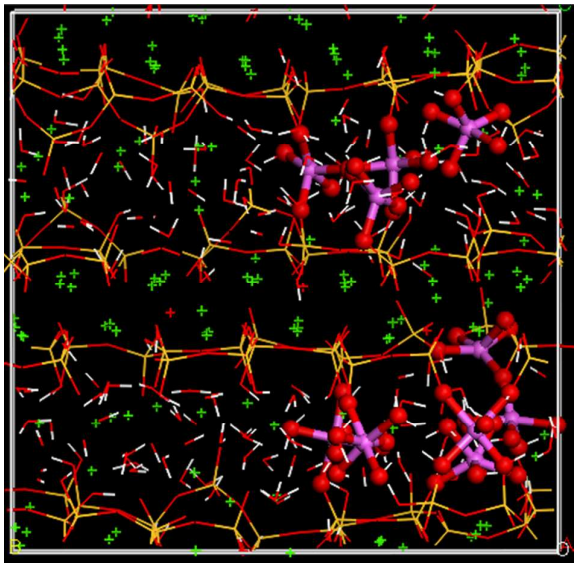

(b)

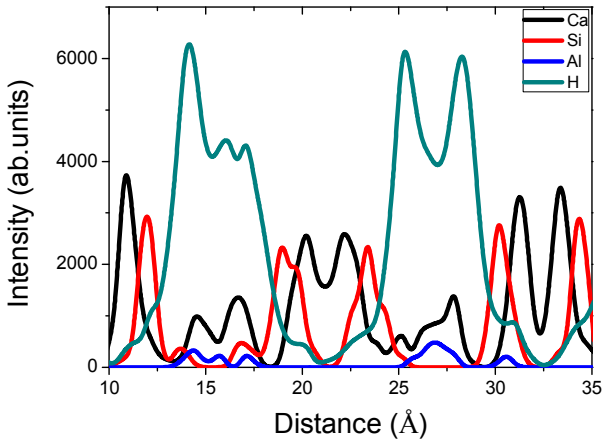

(c)

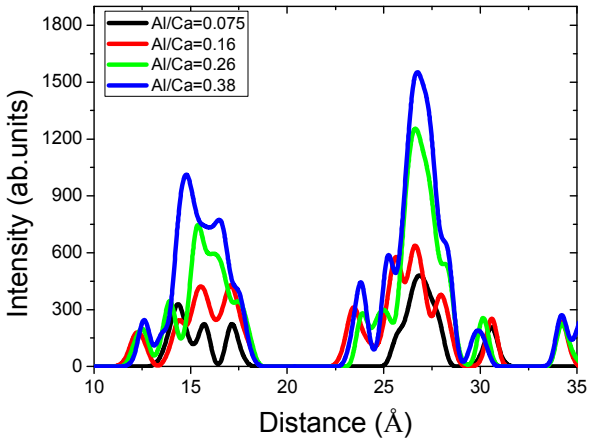

(d)

Fig.2 (a) Molecular structure of C-A-S-H gel with Al/Si ratio 0.075 for Si-Al substitution (b) Molecular structure of C-A-S-H for Al/Ca ratio 0.075 for Ca-Al substitution; red balls represent oxygen atoms and the purple ones are Al atoms; (c) atomic density distribution of Ca, Si, Al, H atoms in the C-A-S-H for Al/Ca ratio 0.075; (d) atomic density distribution of Al in the C-A-S-H gel with Al/Ca ratio of 0.075, 0.16,0.26 and 0.38.

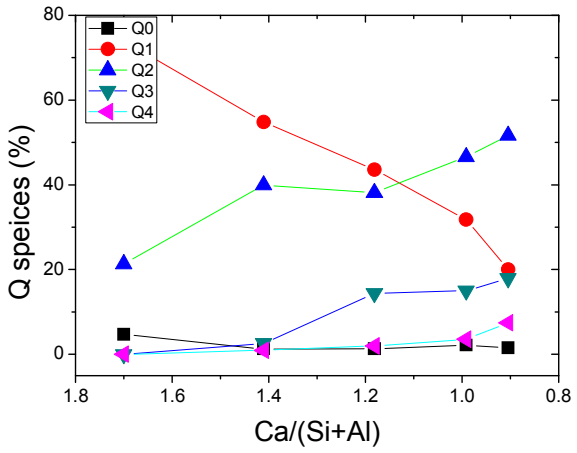

(a)

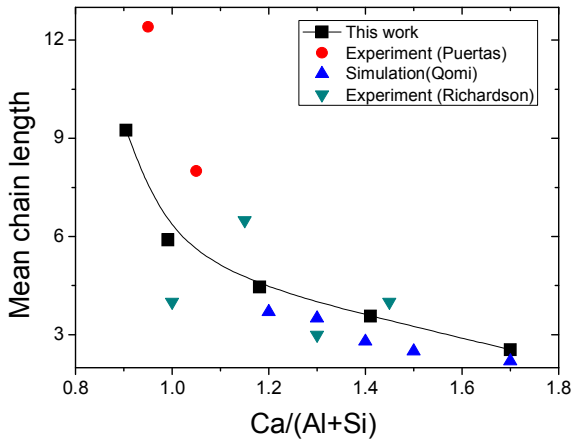

(b)

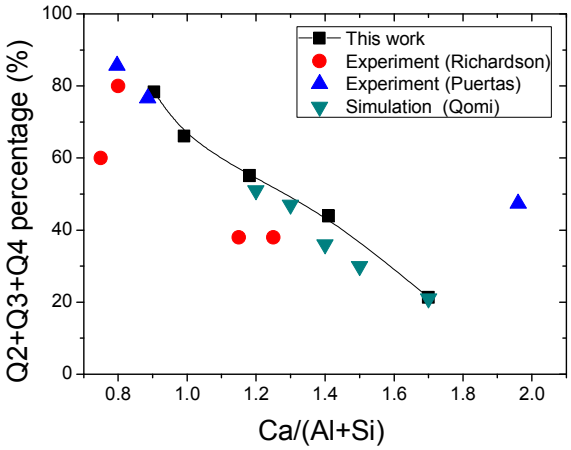

(c)

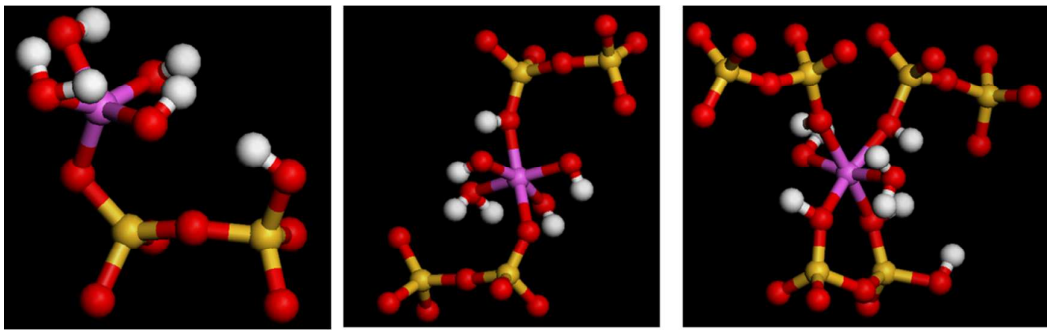

(d)

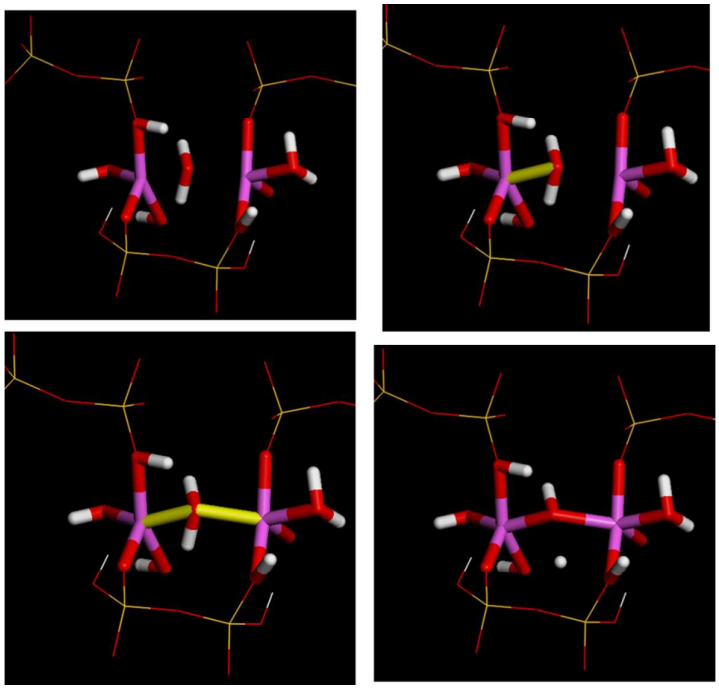

(e)

Fig.3 a. Q_n (n=0, 1, 2, 3, 4) species distribution as a function of Ca/(Al+Si) ratio; b. Mean chain length evolution with Ca/(Al+Si) ratio; c. Percentage of Q_2+Q_3+Q_4 varies with Ca/(Al+Si) ratio; d. Molecular structure formation between Al and defective silicate chains; e. Reaction mechanism for the aluminate species polymerization.

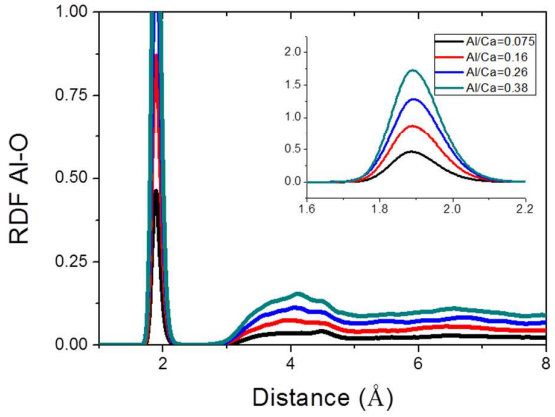

(a)

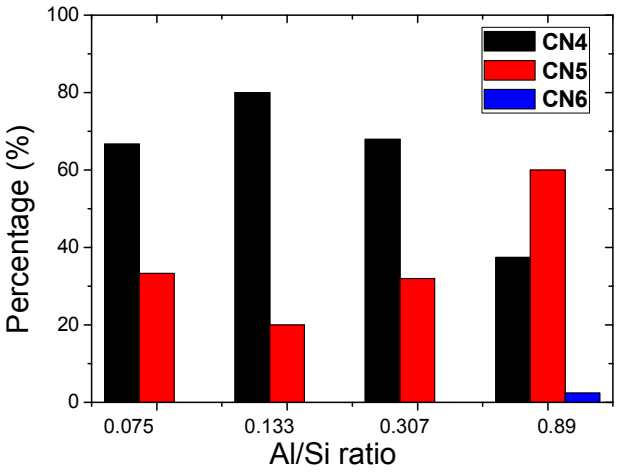

(b)

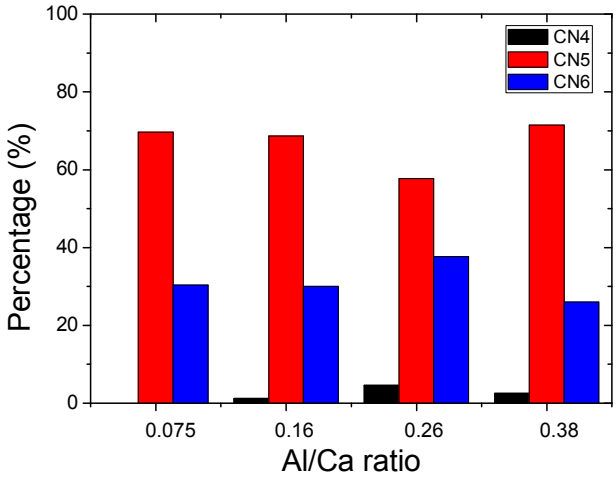

(c)

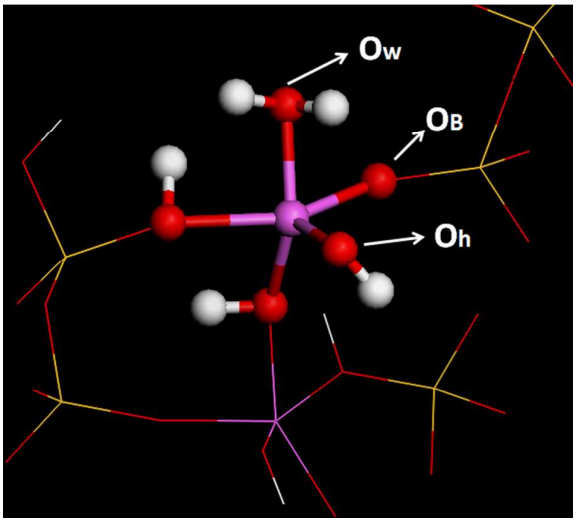

(d)

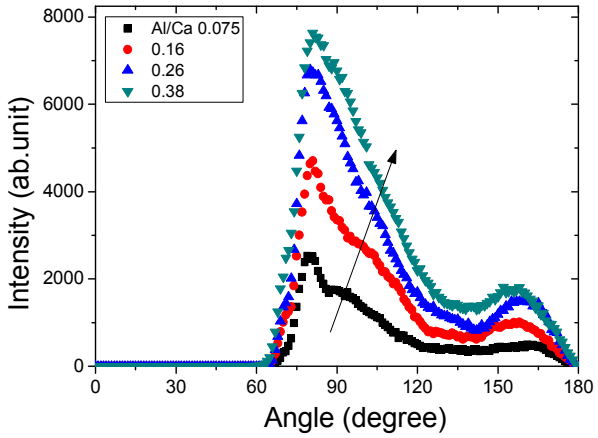

(e)

Fig.4 a. RDF of Al-O at different Al/Ca ratio; b. Coordination number distribution of Al atoms at different Al/Si ratio for Si-Al substitution; c. Coordination number distribution of Al atoms at different Al/Ca ratio for Ca-Al substitution; d. the local structure of an Aluminate octahedron; e. Angle distribution of O-Al-O at different Al/Ca ratios.

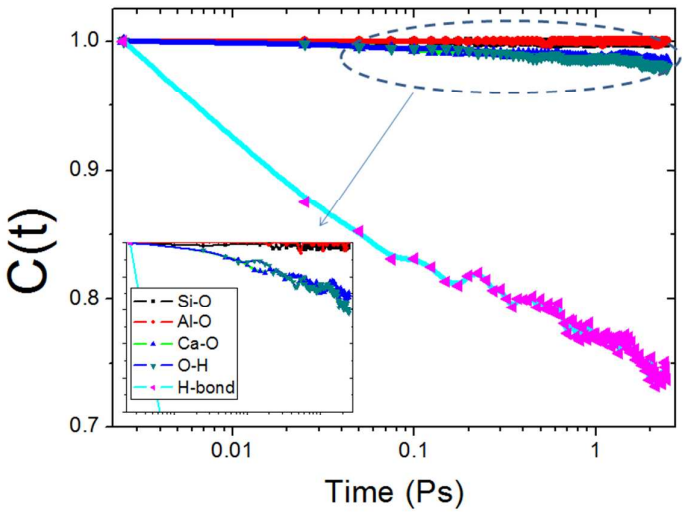

(a)

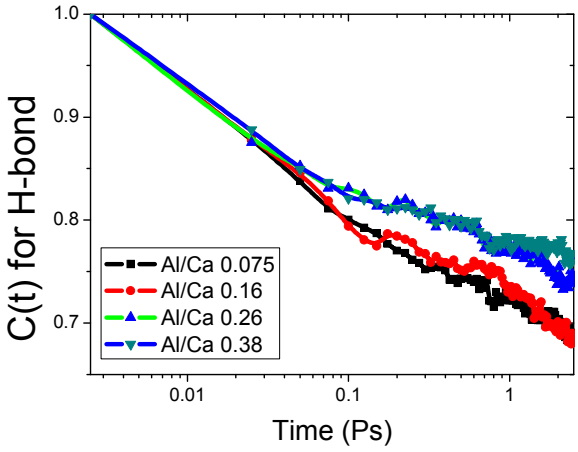

(b)

Fig. 5 a. Time correlated function (TCF or C(t)) of different bonds in the C-A-S-H gel; b. TCF for H-bonds at different Al/Ca ratio.

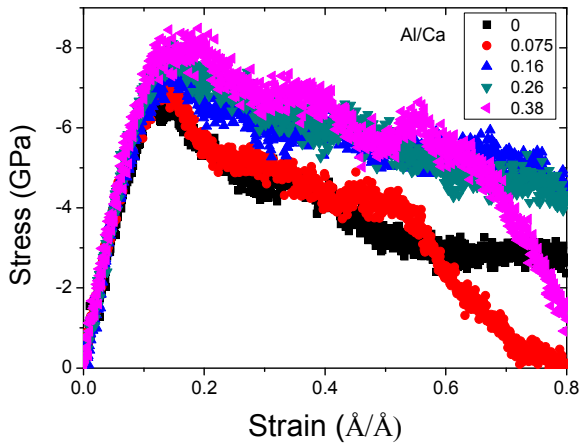

(a)

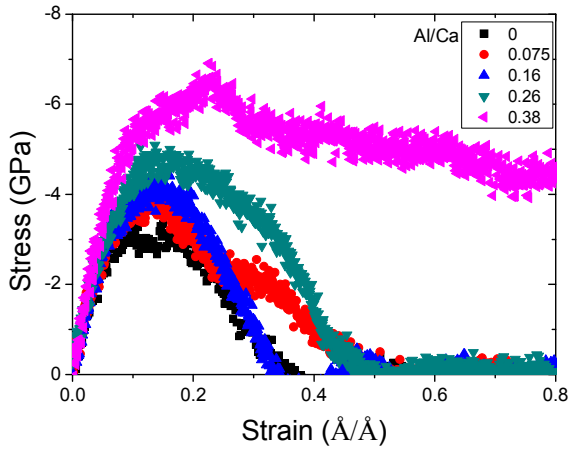

(b)

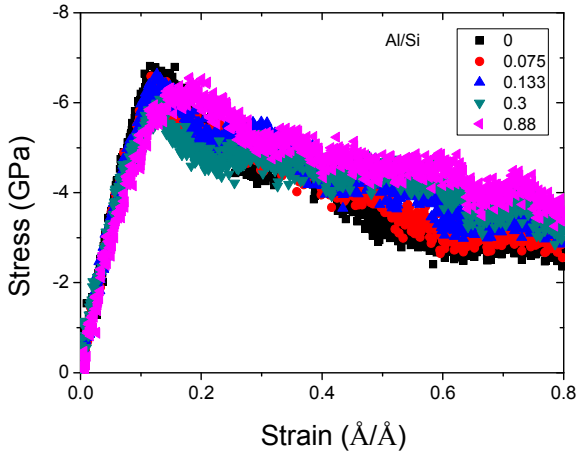

(c)

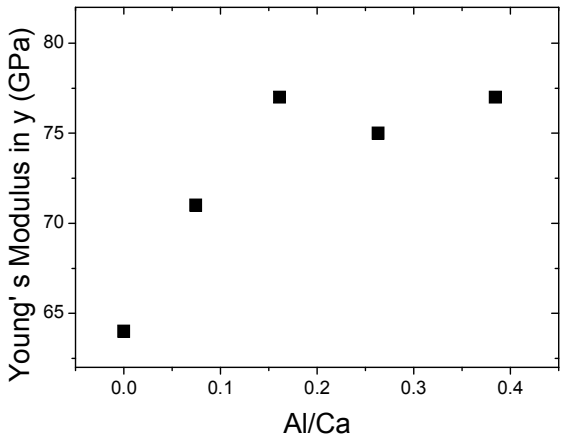

(d)

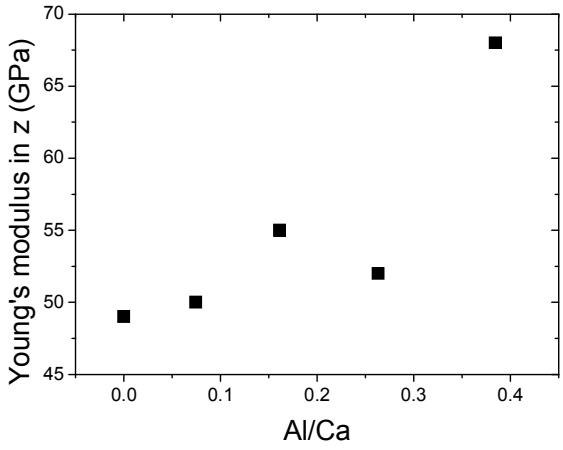

(e)

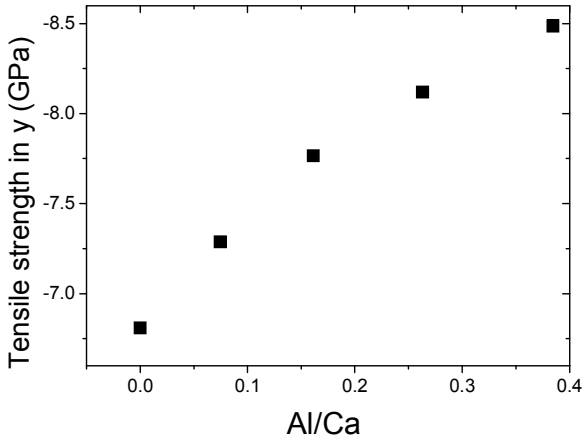

(f)

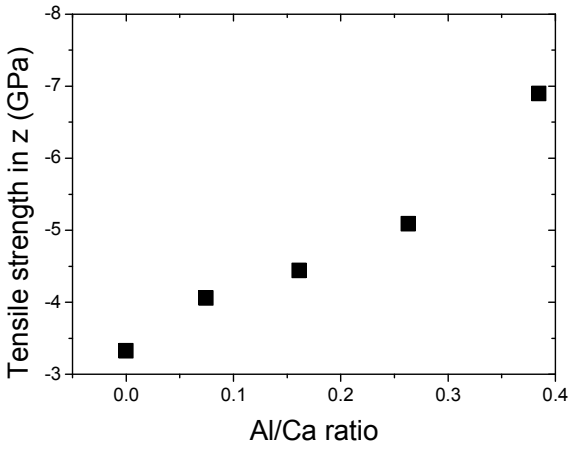

(g)

Fig.6 a. Stress-strain relation along y direction for the Ca-Al substitution; b. stress-strain relation along z direction for the Ca-Al substitution; c. stress-strain relation along y direction for the Si-Al substitution d. Young's modulus in y direction evolution with Al/Ca ratio; e. Young's modulus in z direction evolution with Al/Ca ratio; f. Tensile strength in y direction evolution; g. Tensile strength in z direction evolution.

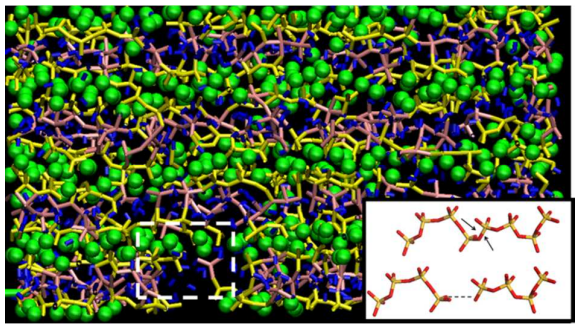

(a)

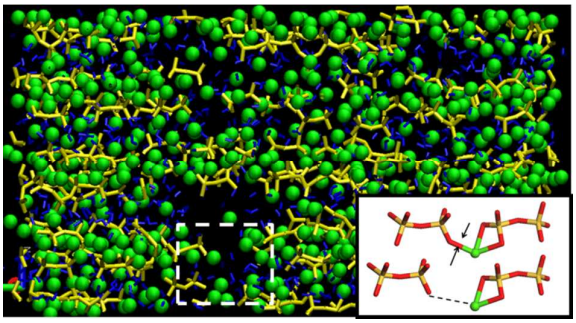

(b)

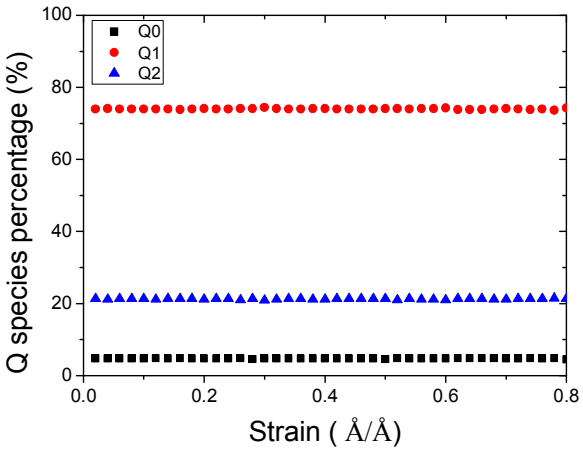

(c)

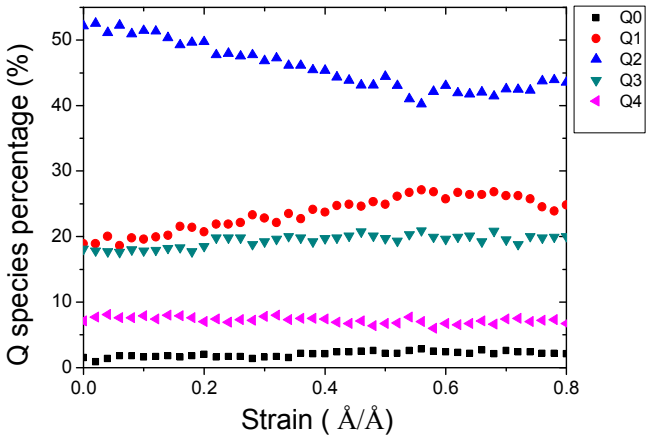

(d)

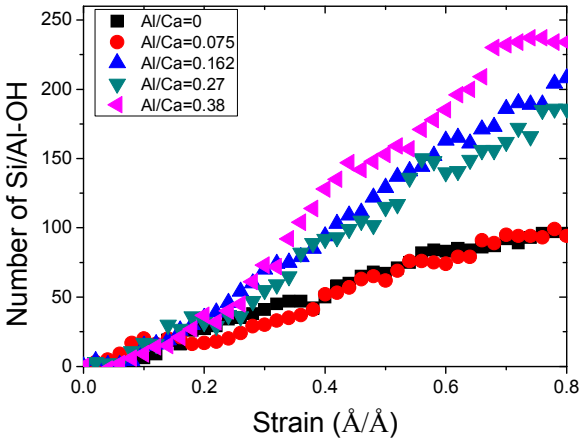

(e)

Fig. 7 a. Molecular structure of deformed C-A-S-H gel at strain 0.4 Å/Å;b. Molecular structure of deformed C-S-H gel at strain 0.4 Å/Å; c. Q species evolution with strain for C-S-H gel; d. Q species evolution with strain for CASH with Al/Ca ratio 0.38; e. hydroxyl evolution at different Al/Ca ratios.

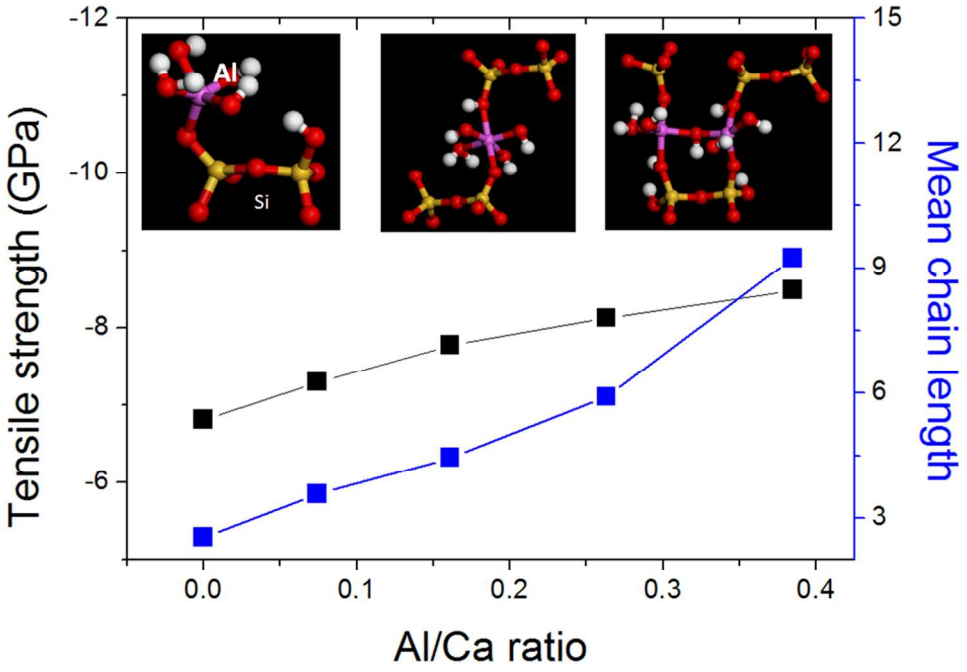

Tensile strength and Mean chain length evolution with the Al/Ca ratio. Yellow-red chains represent the silicate species and purple-red chains are the aluminate species.
291x202mm (96 x 96 DPI)